

3D Optical Scanning of Mechanical Sound Carriers
Technical Description
Revised 6-29-2009

Collaboration

E.W.Cornell, V.Fadeyev*, M.Golden**, C.Haber, R.Nordmeyer,
Lawrence Berkeley National Laboratory

P.Alyea, L.Appelbaum, E.DeAnna, E.Eusman, E.Hansen, D.van der Reyden
The Library of Congress

*now at the University of California, Santa Cruz

**unaffiliated guest

Introduction

This paper discusses the application of optical surface profiling in three dimensions (3D) to the digitization of audio data which are held on mechanical sound carriers. This approach is the basis of the “3D” project supported by the Institute of Museum and Library Services[1]. The original references to this work were published in 2003 [2] and 2005[3]. Additional information is posted the project URL [4] and published [5].

In the 3D process, a probe is used to create a detailed digital topographic map of the surface of a mechanical sound carrier. A numerical algorithm, executed on this map, can be used to emulate the stylus motion, virtually, and reconstruct the recorded sound. This approach is a generalization of the 2D micro-photographic method employed in the IRENE project [4-6] and other photographic methods such as VisualAudio[7]. Imaging in 2D can only resolve certain features of lateral cut recordings. In order to resolve vertically cut recordings, such as Edison cylinders, or the full groove profile in a lateral cut recordings, it is necessary to profile in 3D.

The difference between 2D and 3D imaging is further illustrated in Figure 1. For discs, the 2D imaging used by IRENE provides a subset of the potential information which could be retrieved by a full three dimensional (3D) imaging of a surface. IRENE extracts information from the 2-4 high contrast edge transitions visible at any point (in time) along the groove trajectory. Three dimensional scanning offers the possibility of greater redundancy, and thus higher quality reconstructions, due to the 20-30 points measured.

The geometry of common vertical and lateral cut recordings is also described in Figures 2 and 3. Table 1 lists some of the parameters of mechanical sound carriers. From these parameters it can be concluded that a 2D imaging system would need to have a lateral resolution of ~0.5 micron in order to image coarse groove shellac and lacquer discs (typically “78’s”). Such discs were the dominant recording medium for the first half of the 20th century. For vertically cut cylinders a depth resolution of ~0.1 micron is required. These cylinders were produced both for commercial use and for field recording from the late 19th century through about 1930.

The surface structure of a mechanical carrier can be digitized by an optical probe, contingent upon certain requirements. This probe will measure a region small compared to any significant surface variation. A mechanical carrier holds an analog representation of the cutting tool trajectory. The optical probe acquires object data on a series of discrete points. The imaging of the groove pattern is equivalent to a digital time sampling in the spatial direction analogous to time and a digital pulse height sampling in the direction analogous to stylus amplitude. The digital time sampling is determined by the dimensions of the spot and the spacing between sequential measurements.

Let the spot size be W and the spacing between measured points be D . If the linear surface speed of the record is S , the sampling frequency is given by, $f_{\text{SAMPLING}} = S/D$. In order to satisfy the Nyquist criteria, the digital sampling should be at a frequency at least twice the highest signal tone. In addition, aliasing of higher frequency noise must be avoided. It is observed that if the recording is sampled at a rather high frequency, relative to the sonic content, negligible noise power remains to be aliased.

Methods of high resolution 3D microscopy have been developed to serve the need for precision inspection in such fields as semiconductor wafer processing, micro-machining, optics, and paper and fabric processing. The relevant approaches are based upon either scanning confocal microscopy [8,9] or white light interferometry [10,11]. Studies conducted in the R&D leading to this proposal identified confocal microscopy as the more robust approach being less sensitive to surface slope variations.

The particular scheme used here, extended field color coded confocal microscopy [9], is described in Figure 4. In this scheme, a polychromatic pin-hole source is used and the optics has an exaggerated chromatic aberration. Now each wavelength comes into focus at a different depth and the reflected in-focus signal is analyzed by a spectrometer. This method features similar resolution and spot size as the more common monochromatic laser based systems but may acquire points at a higher rate with stationary optics. Maximum data rates are 4000 Hz per point and depth of field can vary from 20 μm to millimeters. Figures 2 and 3 are examples of images acquired by this method. The parameters of the confocal probes used are given in Table 2. New probes achieve much faster data rates by measuring large numbers of points in parallel on a fixed spatial grid. The properties of a fast probe are also given in Table 2. Such a probe is an obvious choice for any larger scale digitization project and has been studied in the more recent phases of this research. Table 3 summarizes the scan performance expectations for these probes on a variety of representative media.

Scanning and Data Taking

In order to profile a surface, a scan is performed using precision mechanical stages to translate from point-to-point (See Figure 5). If the sample is moving during the measurement the sensor will average over an elongated region of width W ($W = \text{spot size}$) and length $l = v/f$ ($v = \text{stage velocity}$ and $f = \text{data rate}$). The minimum time required to scan a region of size $Area$ using a grid of points with spacing g_x and g_y is given by,

$$T_{SCAN} = (Area / f g_x g_y) + reset \quad (1)$$

There are two modes to consider. In the case of a single point probe, typically x is the direction along the cylinder axis and y is the direction around the cylinder axis. If x is the first scan direction, and the x stage is moving, its velocity v must be $f g_x$. As an example, the minimum time required to cover a 2 inch diameter cylinder with $g_x = 10 \mu\text{m}$, $g_y = 5 \mu\text{m}$ (corresponding to a 96 KHz time sampling) and $f = 1000 \text{ Hz}$ is 81 hours using the CHR probe described in Table 2. Factors of 2 - 4 scan time reduction come with a coarser grid size if allowed. In the case of a multipoint probe, such as the MPLS-180 described in Table 2, $g_x = 1800 \text{ mm}$. The natural scan order is to first rotate the cylinder and then shift the probe by 1.8 mm (overlaps are also possible). As an example, the minimum time required to cover a 2 inch diameter cylinder with $g_y = 5 \mu\text{m}$ (corresponding to a 96 KHz time sampling) and $f = 1000 \text{ Hz}$ is 27 minutes. Again, factors of 2 - 4 scan time reduction come with a coarser azimuthal grid size if allowed. Clearly the MPLS offers a dramatic speed increase. In practice it may be necessary to stop and start the scan periodically in order to control positioning systematics, re-establish a home position, or gather data. In this case an extra term (*reset*) should be added to Eq. 1 to account for this overhead. In the case of a mechanical sound carrier, the point spacing along the groove direction determines

the ultimate sampling frequency. The spacing across the groove contributes to the accuracy with which the groove profile position can be determined at any one time slice.

Measurement and Analysis with a Single Point Probe

To clarify the technical basis a description of a test measurement and its analysis will be given. This measurement was made with the single point probe (CHR) and can be considered as a basic benchmark. In a later section we will compare this with the faster MPLS multipoint probe.

The sample studied was a commercial Edison Blue Amberol cylinder. Other studies have addressed uniquely recorded soft wax cylinders, dictation belts, and disc phonograph records. The Amberol, being relatively common, is useful here since a stylus playback could also be made for comparison.

A confocal probe (Table 2) with a 330 μm range was coupled to custom configured stage movement and read out through a computer. The stages were controlled by DC servo motors and read by linear encoders. The linear stage resolution was 100 nanometers and the accuracy was 2 μm . The setup is shown in Figure 6 for the single point probe.

The surface scanning strategy used was based upon the parameters of the probe and the phonograph record. The cylinder was cut with 200 tracks per inch and a nominal rotation speed of 160 revolutions per minute (r.p.m.). As a matter of convention, “longitudinal” will refer to the direction across the tracks and parallel to the axis of the cylinder. As a matter of convention, “temporal” or “azimuthal” will refer to the direction along the tracks.

The result of a scan is a data set consisting of heights at various lateral and azimuthal positions. From the lateral point set acquired at each azimuthal (temporal) position, a best estimate of the local groove depths can be derived. The lateral sampling interval is determined such that sufficient accuracy is found on the groove depth. The azimuthal sampling interval is determined to provide for sufficient audio time sampling.

For the 200 t.p.i. cylinder technology of the present sample, the groove width is 127 μm , ridge to ridge. The confocal probe spot size used is 7.5 μm and the probe signal averages over a region of area 7.5 μm by f_{gx} during a single measurement. Sufficient points must be acquired across the profile to assess its shape. For the 127 μm pitch, 10 μm between points was judged sufficient, assuming complex damage structures did not need to be resolved.

The grid spacing along the temporal direction determines the digital time sampling. For 160 rpm, a spacing of 0.01° results in a 96 KHz sampling rate, in significant excess of the sonic content recorded on these carriers. Digitization at high sampling frequency also minimizes possible aliasing effects.

The strategy used was to scan along the axis and then increment the azimuth. A typical segment of data acquired along one longitudinal segment is shown in Figure 7.

Figure 8 shows a composite of all the angular scans for a short longitudinal segment. The vertical

scale is exaggerated but a clear deviation from a cylindrical form is seen. The overall deviation is $\sim 250\text{ }\mu\text{m}$. This can be due to surface imperfections and off-center rotation. The structure is at low frequency since the cylinder rotates at 2.67 Hz during a stylus-based playback, and can be reduced by global fitting, low-pass filtering, or other corrections to the data.

For the purpose of analysis, the data is organized into a series of the longitudinal scans, one at each azimuthal position around the cylinder (or disc). To each scan (like Figure 7) a peak and valley finding algorithm is applied to locate all or most of local maxima (ridges) and minima (groove bottoms). Such an algorithm fits second order polynomials to groups of data-points around candidate extrema. A first pass through the data can easily find the real trajectory of the groove (which differs from a simple helix due to distortions of the cylinder and its motion) and the average groove profile. The groove trajectory is parameterized and each extrema can be checked against it. This represents a strategy for finding and rejecting damage or debris on the surface. Furthermore each extrema can be checked for consistency with the groove profile determined from the full data set. For good extrema, a parabolic fit yields the groove depth or the ridge height.

A variety of global corrections can be applied to the data to mitigate the effects of the overall distortions shown, for example, in Figure 8. This is a unique aspect of a full surface profile measurement. The entire data-set is self-calibrating and allows for corrections to low frequency systematics. Such global corrections include subtraction of the average level from each longitudinal scan, and a local (smoothed) ridge to valley subtraction. The latter regards the ridges as a measure of the overall shape of the cylinder while the valleys contain both the sonic content and the overall shape.

Once the corrections have been applied, the local minima are re-ordered as a time sequence following the groove trajectory. This is then a measure of the stylus displacement as a function of time at the raw sampling frequency (in this case 96 KHz). This time series can be differentiated numerically to calculate the stylus vertical velocity, which is proportional to the sound amplitude. The series can be digitally filtered to remove excess frequency content, re-sampled as convenient, and written to an audio file such as WAV format. Optional equalization curves may also be applied to compensate for pre-emphasis in electrical recordings, or for the properties of acoustic recording elements.

Results

To make a comparison with stylus playback, the same cylinder was digitized on a (modern) Archeophone player. This player spun the cylinder with a motor and captured the sound with a Shure V14 cartridge and a KAB Souvenir Pre-amplifier set for mono, a flat frequency correction, and vertical movement. The comparison is shown in Figure 9 left for the optical and raw stylus versions respectively. Figure 9 right shows an expanded view of these same clips. This sample is available at the project URL [4] as well. The comparison is also illustrated in Figure 10 which shows an FFT spectrum analysis for these clips. It is clear that the stylus version contains significantly more low frequency artifacts due to the deformations discussed above.

The figures and clips show that the 3D optical method provides an accurate audio transcription as compared to a stylus playback. The references [3,5] treat additional issues not included here. These include analysis details, extended damage sites, and surface contamination.

No post-processing has been applied to the samples presented here. In principle the sound quality could be enhanced by additional bass boost, and digital de-clicking or noise reduction. (Further examples are presented on the aforementioned website.).

Measurements and Data Taking with the Multipoint Probe

Using the MPLS multipoint probe the scan speed is increased dramatically. This section addresses the performance of a system using the MPLS. Additional analysis and visualization tools were developed to exploit this new capability.

The cylinder scanning apparatus is shown in Figures 11-14. The cylinder is held on a custom designed conical mandrel. The mandrel rotates with a precision direct drive servo motor under the control of computer. The confocal probe is held on a linear motor translation stage which can move it along the cylinder's axis. A third linear actuator varies the distance of the probe from the cylinder and is used to maintain an optimal working distance. This actuator is controlled by a laser displacement sensor which monitors the shape of the cylinder as it rotates.

The confocal probe, referred to as the MPLS180, images a set of 180 points on the surface of the sample. The points lie along a line with a pitch of 10 microns. The total line length is 1.8 mm. Each point has a diameter of 3.5 microns. This is to be contrasted with the original single point probe, referred to as the CHR450, which imaged a 7 micron spot.

In a normal data taking run the probe images an entire rotation of the cylinder and then translates 1.8 mm. Alternate modes have been implemented in which the probe translates by less than 1.8 mm in order to average multiple measurements of the same point or sample the surface at a finer pitch than 10 microns.

The time required to complete a scan depends upon the number of samples taken around the cylinder circumference. A typical value is 20-30 minutes. This, as predicted in the proposal, is a dramatic and overwhelming improvement relative to the single point CHR450 process.

The measurement process is controlled by a software application known as "3D-Control" and written in LabView 8.2. The application front panel or GUI is shown in Figure 15. From the front panel the user can set the scan parameters (probe rate, start and stop position, translation step, time sampling, data file path), view a sample of the data and various statistical measures, and monitor the progress of a scan. This interface is prototypical of what would be provided in a production style machine.

Once a measurement is complete the data is saved in a binary file. A data format has been defined which consists of a header, containing scan parameters, followed by a list of the measured points. Typical size is 700 Mbytes for a 3 minute cylinder sampled at 48 KHz. A naming convention for these data files has been defined which summarizes the measurement as

well. The binary files are read and analyzed by a separate application referred to as “PRISM”. This application is written in Microsoft C#. Part of the application front panel or GUI is shown in Figure 16. PRISM offers the control of many detailed features of the analysis in order to test a range of algorithms, filters, and data manipulations. PRISM can process files collected with the MPLS180 as well as older files collected with the CHR450 which predate this project. Once the raw data has been read, PRISM executes a tracking algorithm in order to determine the trajectory of the groove through the image. This represents the average path a stylus would have followed around the cylinder. The audio content stored in the depth of the groove, at each point in time, and this is defined redundantly by all points along the groove profile. PRISM determines the audio content by comparing most of the points along the profiles to their corresponding positions in the next adjacent time slice and then averaging across the profile. This approach is relatively independent of any model of the groove shape.

PRISM includes a grayscale display of the collected data both overall and in zoomed detail. A cursor allows the user to view the local profile laterally or in the time directions. This is shown in Figure 16. The reconstructed audio may also be view graphically and sampled using an embedded media player.

PRISM contains a number of powerful filtering and data selection features. The “flat” correction removes low frequency data due to deformations of the cylinder shape. This is done by averaging the cylinder shape over many samples and then subtracting this average shape from the data. The effect of the flat subtraction is shown in Figure 17. The “blob” correction finds non-groove like features in the data (dirt, scratches, etc), subtracts them from the image, and then interpolates across the deleted sections. Corrections are applied optionally and may be modulated by setting various parameters. An important aspect of the ongoing work is to determine optimal settings for some of these parameters.

Some aspects of the MPLS performance are summarized below.

1. The depth resolution of the MPLS180 is about 120 nanometers as compared to 20-30 nanometers for the CHR450. *This is clearly visible as a graininess in the grayscale images but apparently has little effect of the broadband noise level in the audio. See comparison of spectra in Figure 18-21.*
2. The depth of field of the MPLS180 is about 400 microns as compared to 330 microns for the CHR450. *While larger, it is insufficient to capture an entire cylinder without adjustment of the position of the probe relative to the sample. This is due to the natural deformations of the (old) media. To deal with this we implemented a laser displacement sensor control loop driving the probe distance (“autofocus system” Figures 13). The procedure works well but does add some small but measurable noise (Figure 22) to the audio due to the continuous motion of the probe. We foresee upgrading to a linear motor stage for the probe displacement in order to minimize this.*
3. There are a number of consistently noisy fibers in the MPLS180. *The manufacturer has proposed a cleaning procedure which we have yet to attempt.*

4. Data quality is roughly independent of exposure time as long as intensity is sufficient. *We are seeking to optimize our settings.*
5. Point-to-point, MPLS180 data is much more variable than CHR450 data on the same media samples and this variation is stable and reproducible (it is not random noise). *The scale of the variation is ~ 1 micron, considerably larger than the resolution. This effect is illustrated in Figures 23 and 24 which compare CHR450 and MPLS180 data on the same cylinder. Interestingly this variability has little effect on the broadband audio noise or signal quality. This is because we can determine the audio by differencing each point along the groove trajectory in the time direction, rather than rely on a local parabolic fit. However it can complicate the identification and removal of discrete features ("clicks and pops") somewhat. A more detailed surface scan is shown in Figure 25.*
6. Other media: Beyond cylinders the confocal scanning is of interest for discs and dictation belts, both of which have lateral, rather than vertical groove modulation. *For discs an evaluation is still underway [12,13]. We tested the MPLS180 on dictation belts. These are transparent plastic surfaces. With the CHR450 we were able to scan these using an internal software feature called "2 peak mode". The MPLS180 software initially lacked this feature but the manufacturer has since added it, at our request.*
7. Pilot Study and Comparisons: All eleven cylinders from the Hearst Museum collection have been scanned and analyzed. A portion of each was also scanned with the original CHR. *Some comparisons are seen in Figure 11 and 12.*

Application to Disc Scanning

The technical study described above was based upon measurements of cylinders. As shown in Figure 3 the disc groove walls are considerably steeper than that of a cylinder. For this reason the confocal probe has to be run at a slower measurement rate. This leads to the longer scan times listed in Table 3. Disc scanning involves a number of further optimizations which involve trade-offs between probe rate, grid size, and data collection strategy. Some of these are explored further in referenced documents [3]. The greater redundancy of the 3D data set leads to the stated potential for higher precision and higher fidelity audio capture. In Figure 26, the confocal probe deployed in a disc scan configuration is shown. A recent report on disc scanning was written [12], and earlier relevant study was done [13], and another significant study is underway using the MPLS probe.

Application to Condition Assessment

In addition to audio extraction, the scanning technology studied here can provide a detailed assessment of the condition of mechanical sound carriers. Considering the findings of the Heritage Health Index [13] which report a large fraction of sound recordings are in unknown condition, this may be a valuable capability as well. By collecting high resolution digital images of the carriers, analyses may be executed to identify and quantify features and defects in the sample. An example of this is shown in Figure 27 which details features measured from a variety of recorded sound carriers using the confocal optical scanning technology.

- [1] **Development of a 3D Optical Scanner for Mechanical Sound Carriers**, submitted to IMLS, April 2007
- [2] V.Fadeyev and C. Haber, **J. Audio Eng. Soc.**, vol. 51, no.12, pp.1172-1185 (2003 Dec.).
- [3] V. Fadeyev et al, **J. Audio Eng. Soc.**, vol. 53, no.6, pp.485-508 (2005 June).
- [4] <http://irene.lbl.gov/> contains recent presentations
- [5] E.W.Cornell et al, **Nucl. Inst. Meth. A**, 579 (2007) 901–904
- [6] **IRENE Proposal**, submitted to NEH July 2004 PA 51170
- [7] Stotzer, S., et al., **Digital Signal Processing**, Volume 17, Issue 2, 433-450, (2007)
- [8] Corle, T.R., and Kino, G.S., **Confocal Scanning Optical Microscopy and Related Imaging Systems**, Academic Press, San Diego, 1996
- [9] Cohen-Saban, J. et al, **Proc. SPIE**, 4449, 178-183, (2001)
- [10] Davidson, M. et al, **Proc. SPIE**, 775, 233-247, 1987
- [11] Caber, P.J., **Applied Optics** 32, 3438-3441 (1993)
- [12] J.N. Lutz and M. Yerly, **Studies of Mechanical Recording Media with 3D Surface Profiling Methods: Data Collection and Analysis**, Diploma Thesis, Computer Science Department, University of Applied Science, Fribourg, Switzerland, October 2005,
- [13] S. Nowak and S. Hezel, **Extraction of Sound Using 3D**, Diploma Thesis, Electrical Engineering Department, University of Applied Science, Fribourg, Switzerland, October 2008,

Tables

Table 1: Parameters of various mechanical sound carriers.

Parameter	Coarse	Micro-Groove	Cylinder
Diameter (inches)	10-12	12	2-5
Revolutions per minute	78.26	33.3333	80-160
Groove width at top	150-200 μm	25-75 μm	variable
Tracks/inch (mm)	96-136 (3.78-5.35)	200-300 (7.87-11.81)	100-200 (3.94-7.87)
Track spacing	175-250 μm	84-125 μm	125-250 μm
Fixed Groove depth	40-80 μm	25-32 μm	NA
Ref level peak velocity@1kHz	7 cm/s	7 cm/s (11 μm)	unknown
Maximum groove amplitude	100-125 μm	38-50 μm	~10 μm
Noise level below ref, S/N	17-37 dB	50 dB	unknown
Dynamic range	30-50 dB	56 dB	unknown
Groove max ampl@noise level	1.6 - 0.16 μm	0.035 μm	< 1 μm
Max/Min radii (mm)	120.65/47.63	146.05/60.33	fixed
Area containing audio data	38600 mm^2	55650 mm^2	16200 mm^2 (2'')
Total length of groove (meters)	152	437	64-128

Table 2: Parameters of the confocal probe.

Parameter	1st Generation Probe	New Fast Probe
Probe Model	CHR450 mfg. by STIL SA,	MPLS-180
Measurement Range	330 μm – 1 mm	400 μm
Spot size	7.5 μm	3.5 μm
Sampling Frequency	100-4000 Hz	100-1800 Hz per point
Vertical Resolution	10 - 100 nanometers	120 nanometers
Vertical Accuracy	100 nanometers	same
Points per measm't	1	180
Point spacing	Determined by stage motion	10 μm

Table 3: Examples of representative carriers, parameters, and minimum scan times for various settings, 96 and 12 KHz refer to two extreme time sampling choices.

Format	cylinder	cylinder	disc	dictation belt
Material	molded	Soft wax	Shellac, lacquer	plastic
Dates	1912-1929	Late 1890s +	1910-1950	1950-1970
Method	commercial	unique	Commercial or unique	unique
Content	performance	Spoken word, performance, fieldwork	Performance, fieldwork, radio, commercial	Spoken word
Play time	4 minutes	4 minutes	3 minutes	15 minutes
rpm	160	90	78.26	42
Tracks/inch	200	100	100	170
Confocal rate	1000 Hz	1000 Hz	500 Hz	2000 Hz
Lateral grid*	10 microns	20 microns	5 microns	5 microns
Scan time minutes				
96 KHz	30	55	170	120
12 KHz	3	8	17	12

Figures

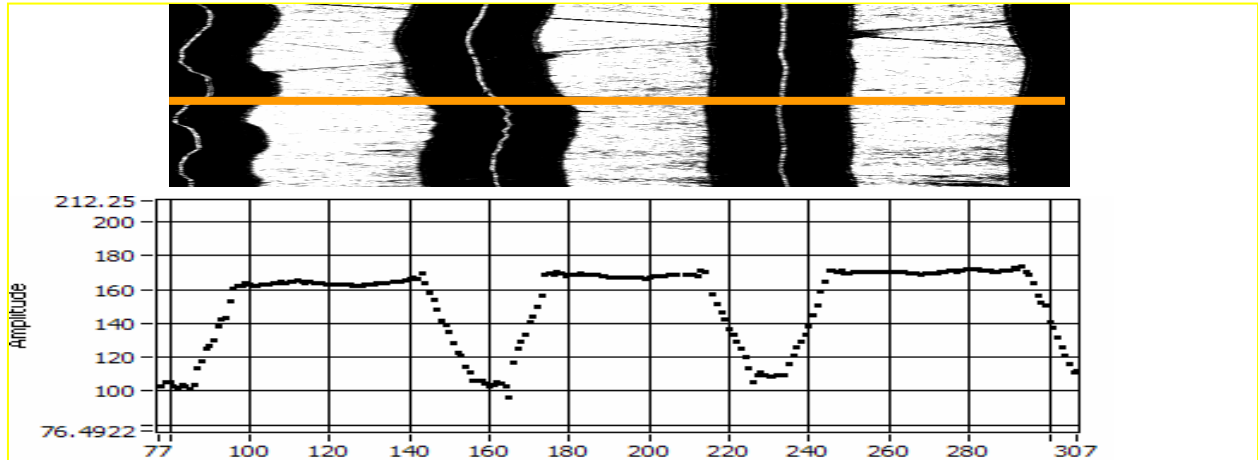


Figure 1 : Upper plot shows a 2D disc image acquired with IRENE. Audio content is extracted from sharp contrast features seen in the image, particularly the dark to light transitions which occur along the groove bottom.. Lower plot shows a 3D scan for one time slice (represented by the orange line). IRENE extracts data from significantly fewer points as there are at most four high contrast edges per track per time slice. 3D can benefit from the redundancy of 20-30 measurement points.

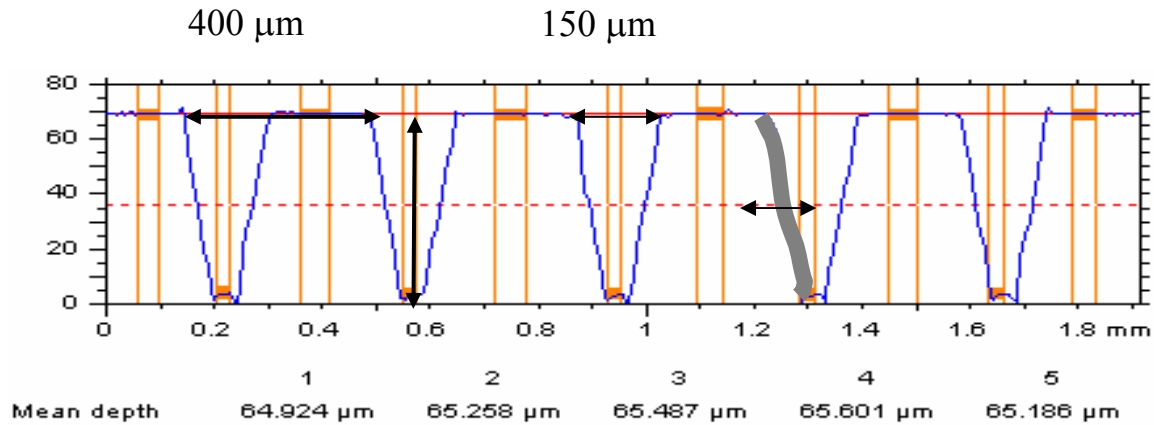
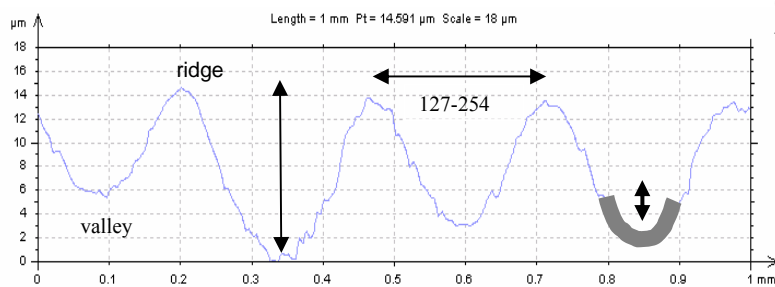


Figure 2: Description of the lateral cut disc record. Top left is an image of a disc. Top center shows a stylus riding in the spiral groove. Top right is a photomicrograph of the groove about 0.75 mm across. The wide white regions are the record surface. The black are the groove walls which slope at 45 degrees. The narrow white line is the groove bottom. Lower plot shows a cross section of the groove. Vertical scale is in microns, horizontal scale is in millimeters. Sound is encoded in the left to right movement of the groove.



Cylinder surface
Vertical cut

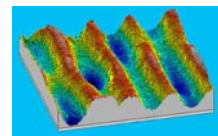


Figure 3: Description of the vertical cut cylinder record. Top left is an image of a cylinder. Center shows a cross section of the groove. Vertical scale is in microns, horizontal scale is in millimeters. Sound is encoded in the vertical movement of the groove. Image at right is a composite of a series of profiles, about 1 x 1 mm square.

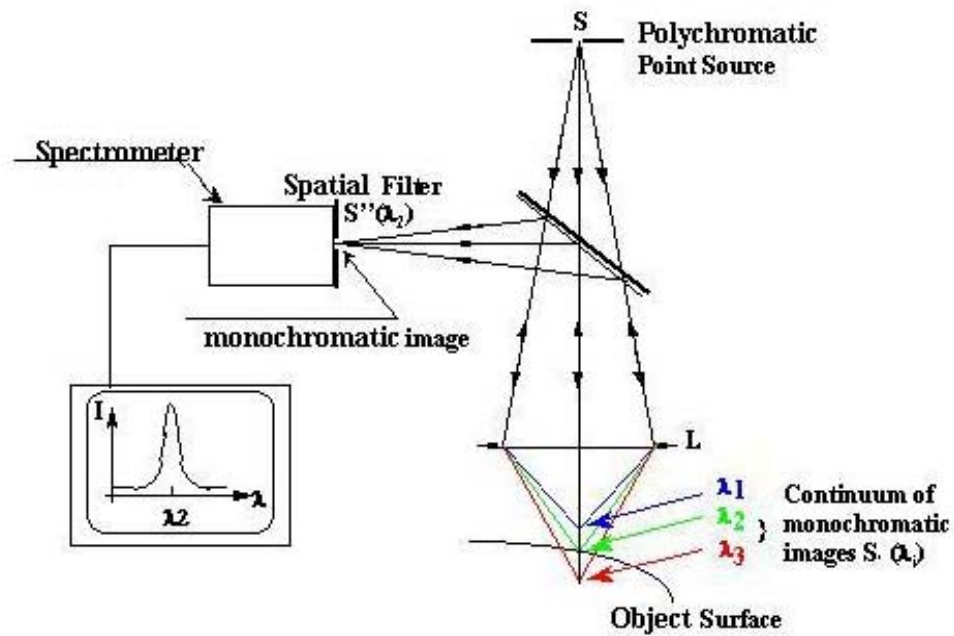
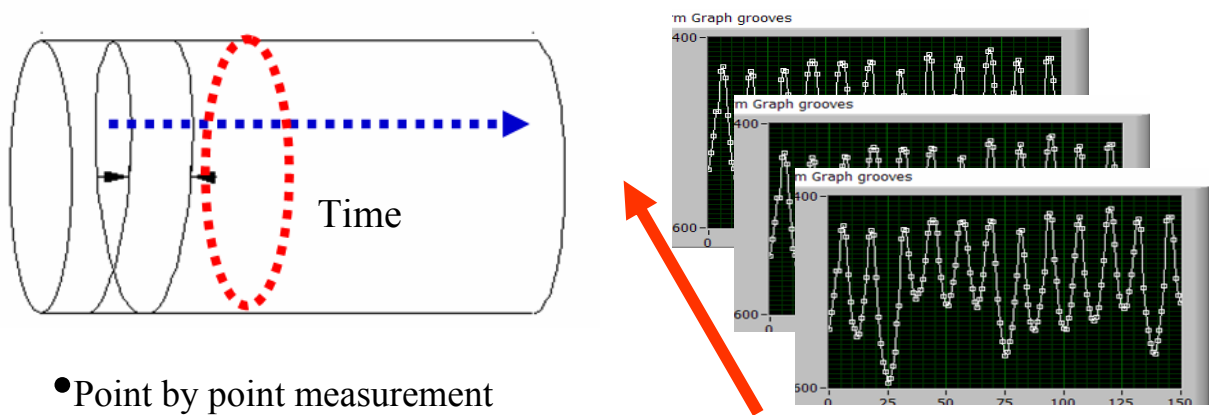


Figure 4: Basic concept of color-coded confocal microscopy. The lens at position L has a large chromatic aberration causing the three wavelengths shown to focus at different depths. Figure is courtesy of STIL SA, used by permission.



- Point by point measurement
- Exposure time per point
- Grid along time direction (red) = digital sampling
 - 0.02 degree = 18,000 samples = 48 KHz
- Grid along axis direction (blue) = points per profile
 - Typically 5 – 10 microns
- 1 probe: ~ 80 hours for 2-4 minutes of audio
- 180 probes: ~ 20 minutes (new multi-fiber probes)

Figure 5: Principle of the confocal depth scan. The red circle represents a scan around the circumference which is executed first. After the circumferential scan, the probe is translated along the axis of the cylinder and the process is repeated. With the original single point probe (CHR450) the surface was scanned point-by-point in this manner. With the new multipoint probe (MPLS180), each circumferential scan covers 180 points separated by 10 microns parallel to the cylinder axis. A few of these are represented by the images at upper right in the figure. The probe is then translated, typically, by 1.8 mm (180 points \times 10 microns). The probe may be translated by smaller increments in order to cover the surface with a finer spacing than 10 microns. During the circumferential scan, the exposure time of the probe and the rotational speed of the cylinder determine the angular spacing between measurements. This then determines the digital time sampling of the measured audio waveform.

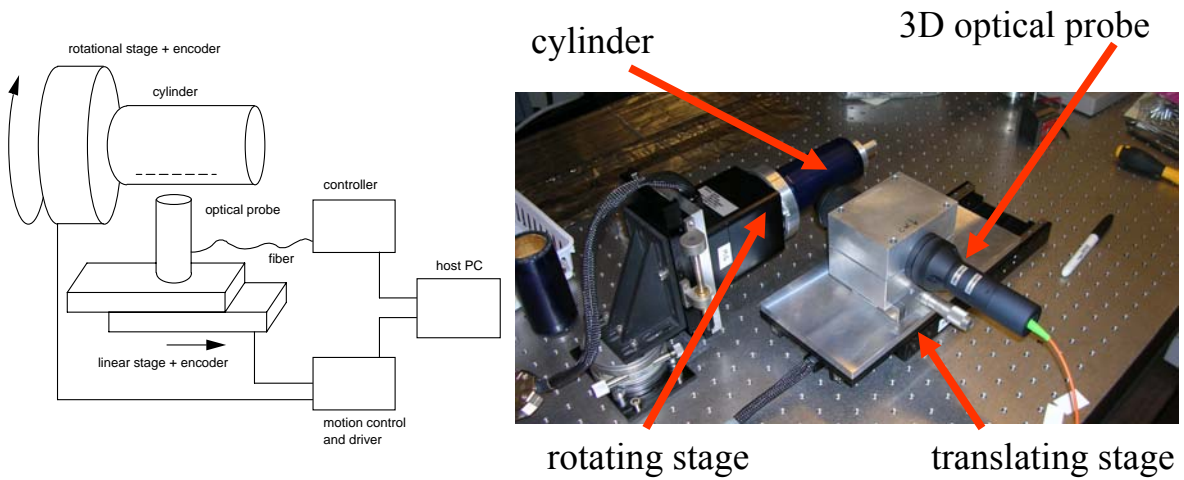


Figure 6: Photograph of the actual scanning apparatus. The controller and CPU are outside the frame.

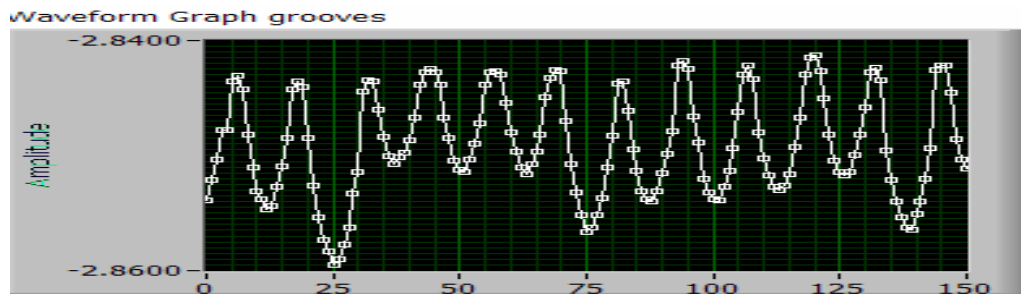


Figure 7: Segment of linear scan along the cylinder axis for fixed angular position. The horizontal separation between points is 10 microns. The vertical scale is millimeters.

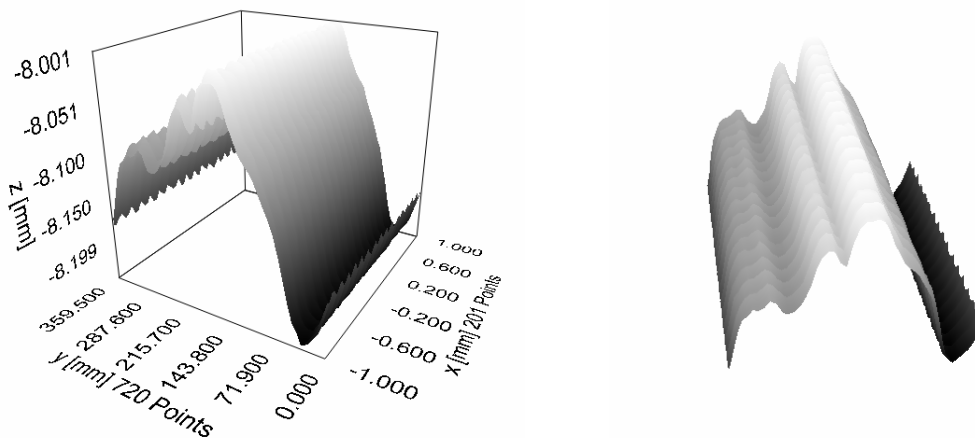


Figure 8: Plots shows 20% of the data scan “unrolled”, two views. Left-right axis (y) is angle from 0 to 360 degrees, axis into the page (x) is position along the cylinder axis in mm, vertical axis (z) is surface height (from a reference point) in mm. A perfect cylinder would be flat at a fixed z position. Instead the surface differs from flat by about 250 μm . This low frequency

structure can be due to a combination of shape imperfection, and off-axis rotation.

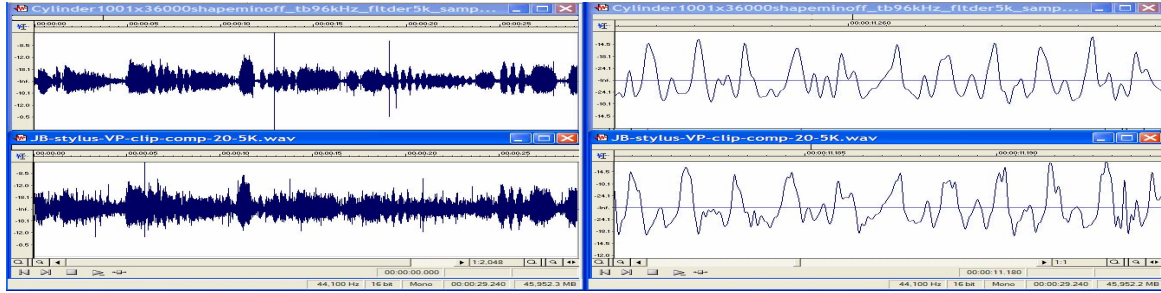


Figure 9: Left top shows 3D optical audio extraction, left bottom shows stylus playback of the same cylinder. Approximately 29 s of audio is shown. Right top is the same data as left top but expanded to show a segment of length 14 milliseconds beginning at 11.254 s from the start of the clip, right bottom is the corresponding section from the stylus version.

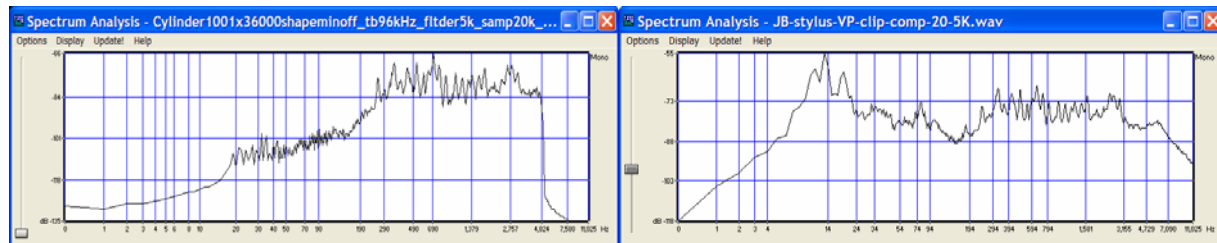


Figure 10: Left, FFT of 3D optical data as in Figure 9 top, and right FFT spectrum analysis of stylus playback. Low frequency artifacts have been suppressed by the global



Figure 11: Overall view of cylinder scanner. Cylinder, in foreground, is held on mandrel and rotated by stage (marked with circular scale). Probe enters from right and is held on linear translation stage (lower right). Laser displacement sensor scans cylinder from above (marked with yellow safety tag).



Figure 12: MPLS180 probe is fed by this console which contains Xenon light source and optical processor. Black cable contains 180 plastic fibers.



Figure 13: Detailed view of laser displacement sensor. MPLS180 can be seen entering from lower right.



Figure 14: Front lens of MPLS180 is seen here imaging the side of the cylinder. Red spot at top is from the laser displacement sensor.

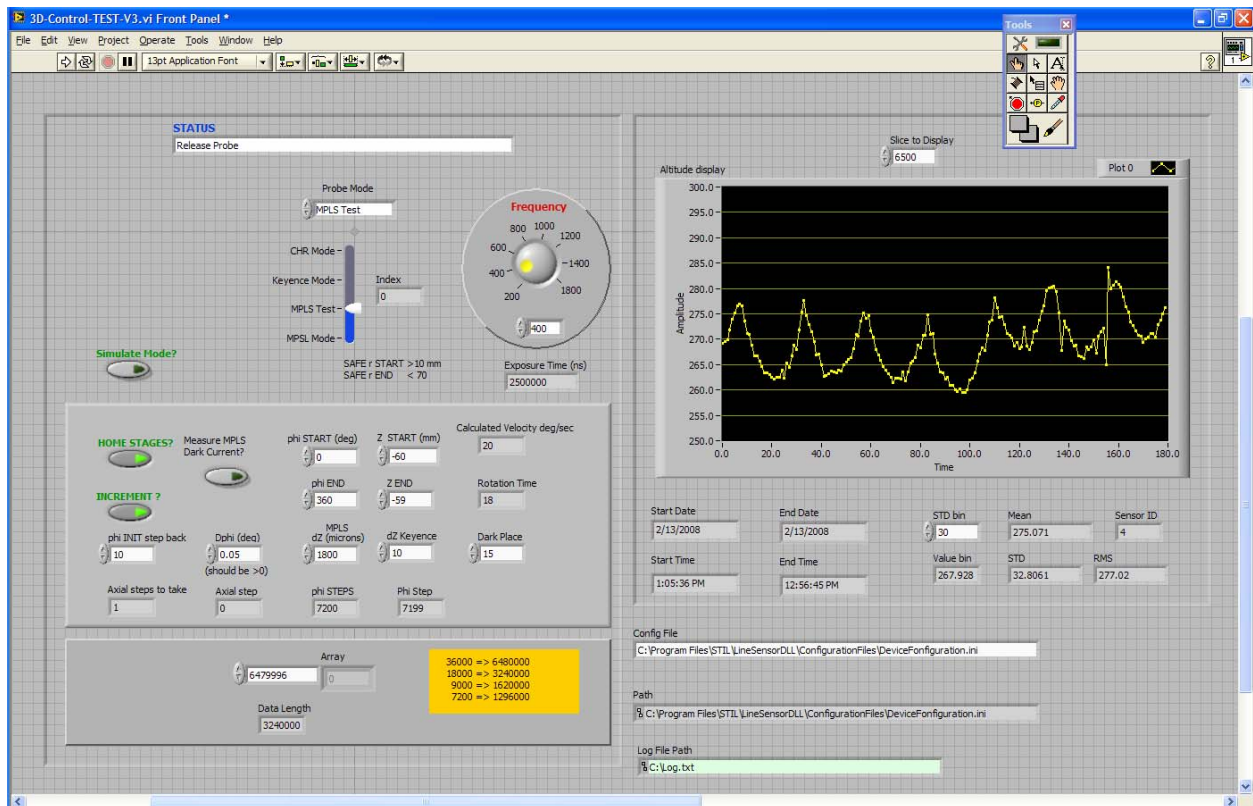


Figure 15: Front panel of the 3D-Control program user interface. Settable parameters and scan progress are at left. Samples of the data and statistical monitors are at right.

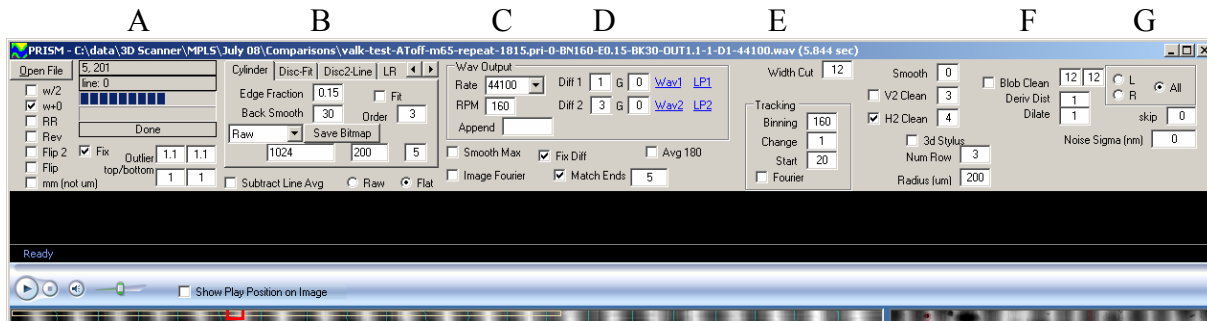


Figure 16: PRISM analysis software control under interface. Controls and status are available to the user from this panel. From the left, processing status is shown by the blue bar A, a set of tabs selects the media format (Cylinder, Disc,...) B, the type of processing (see Figure 19) to view can be selected, the output sampling frequency C and filtering options D-G, and embedded audio player H.

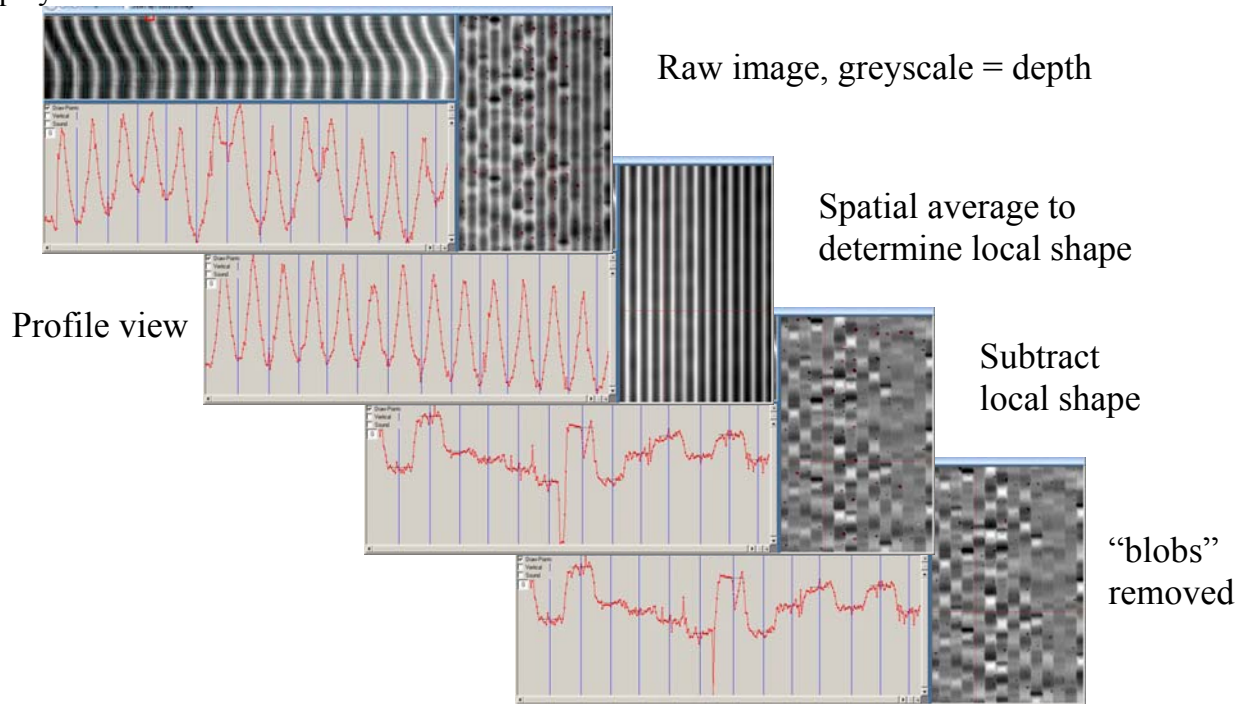


Figure 17: Different analysis options may be displayed or invoked by the PRISM code. Depth is indicated by grayscale. At top left is the raw data subframe, comprising a summary view of the entire data sent (top left within the subframe), a detailed selected region (right within the subframe), and a selected profile from the selected region (lower left within the subframe). Options for the the profile include a view across the profile or along the time direction, display of all measured points, and a display of the extracted audio waveform. The next subframe shows the averaged shape of the cylinder obtained by binning the data into a coarse grid. The third subframe is the difference between raw and averaged. This emphasizes the audio content. Finally in the fourth subframe “blobs”, meaning dust and scratches etc, have been isolated and subtracted from the image.

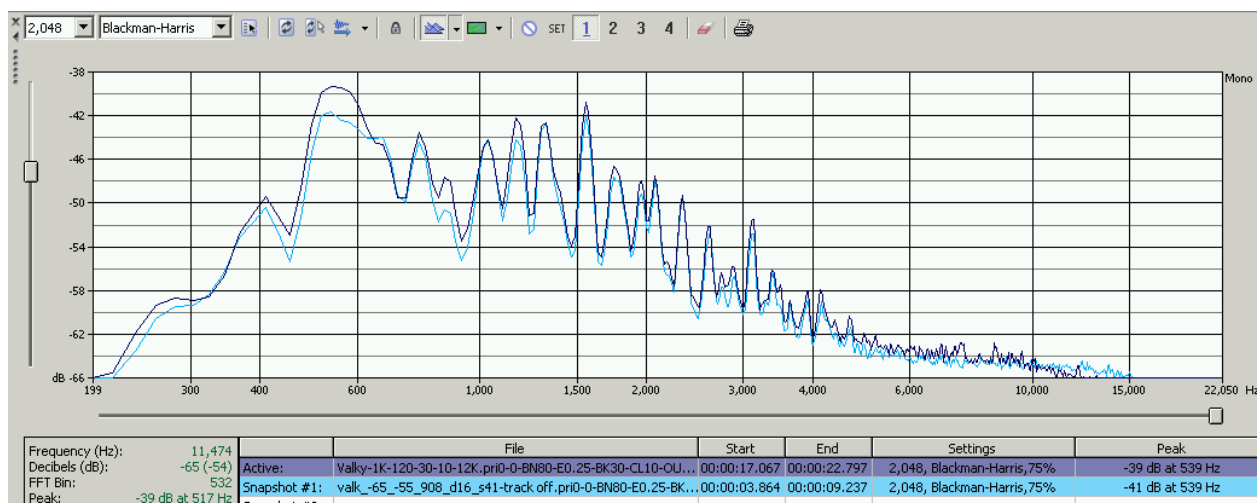


Figure 18: Comparison of CHR450 data (black curve) and MPLS180 data (blue curve) versus frequency on a commercially produced cylinder (in good condition).

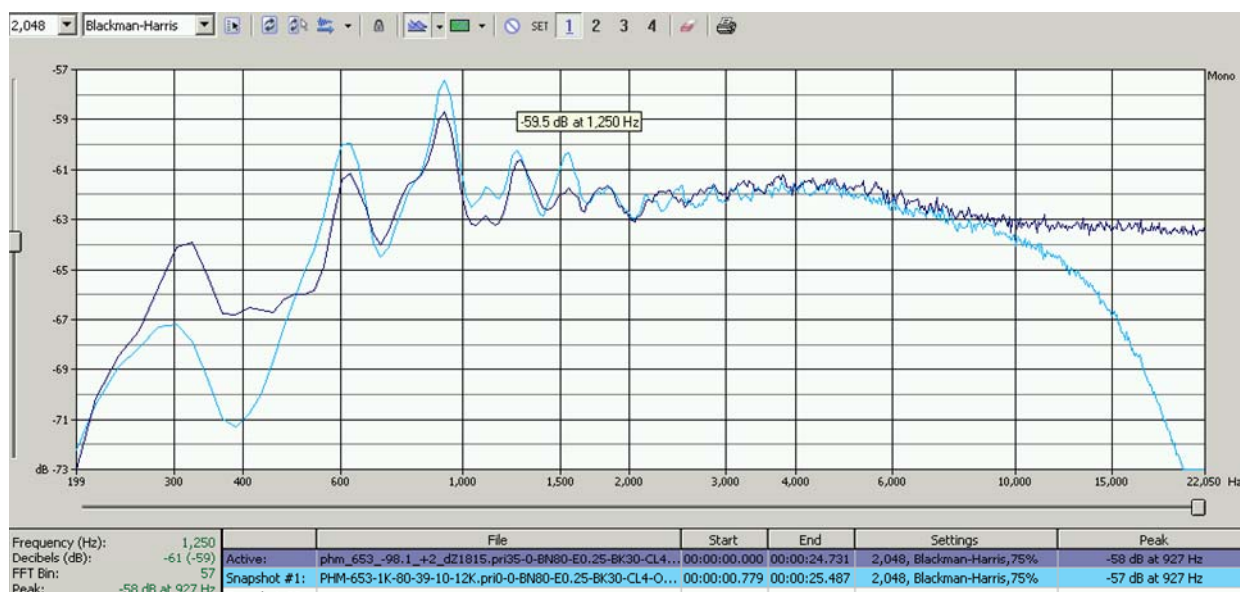


Figure 19: see Figure 20.

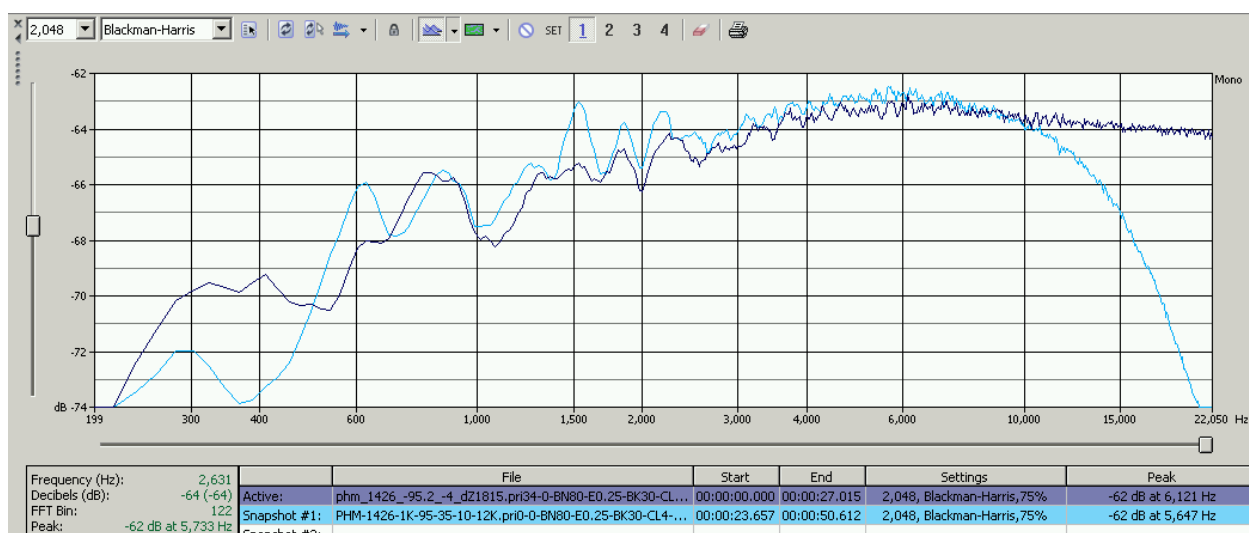


Figure 20: Comparison of CHR450 data (blue curve) and MPLS180 data (black curve). This data is taken on field recorded soft wax cylinders from the Hearst Museum collection. The roll-off seen above 10,000 Hz in the CHR450 data is due to different sampling rates and filters in the analysis and is not relevant to the comparison. Both comparisons (Figure 21 and 22) show a discrepancy at 1500 Hz. While not understood, this may be a parasitic noise structure in the CHR450 data since it appears in both samples.



Figure 21: Comparison of broadband noise (spectra from a “quiet” section) between CHR450 (light blue curve) and MPLS180 (dark blue curve) from soft wax field recorded cylinder (PHM-653). This demonstrates that the lower depth resolution of the MPLS180 does not add appreciable random noise to the extracted audio waveform.

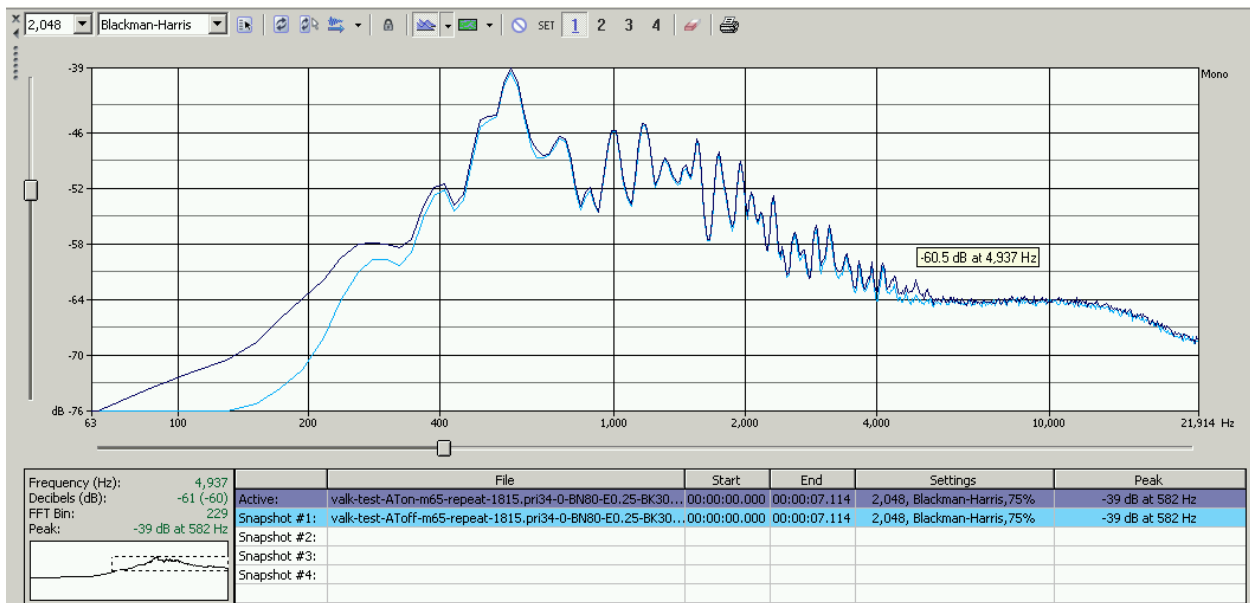


Figure 22: Comparison of MPLS180 data taken with (black curve) and without (blue curve) the laser sensor driving the autofocus motor. The extra noise appears at low frequency and may be minimized with a higher performance stage.

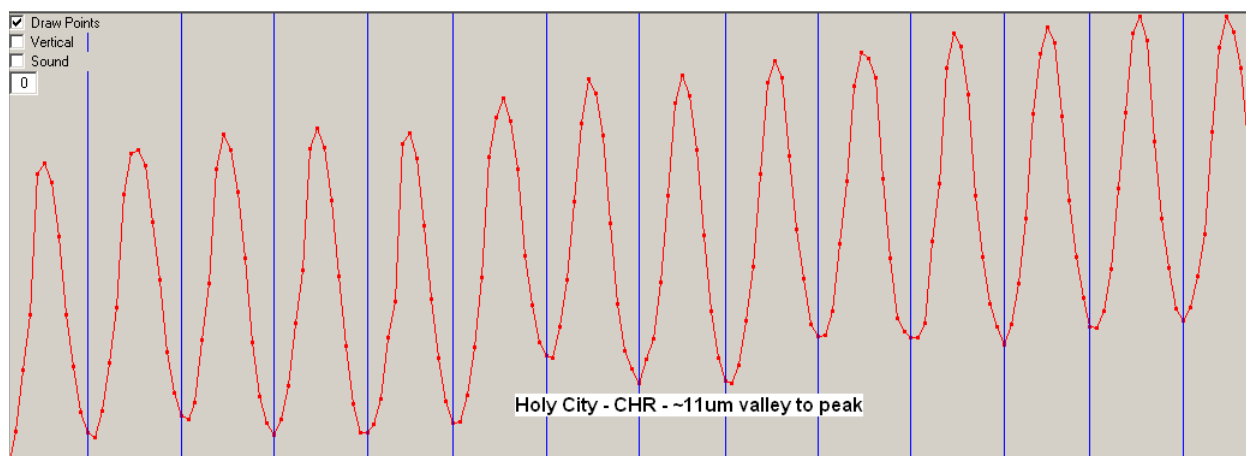


Figure 23: Confocal scan using the original single point probe (CHR450). The vertical axis is depth. The horizontal axis is position along the cylinder axis. Lateral (left-to-right) spacing of measurements is 10 microns.

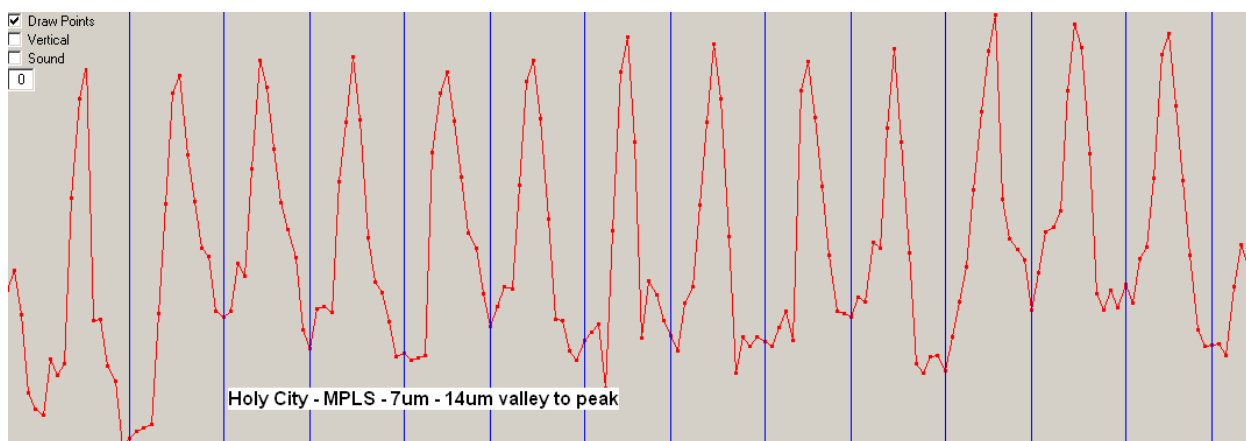


Figure 24: Confocal scan using the new MPLS180 multipoint probe. Same material as shown in Figure 23. The observed variation (lack of smoothness) is not random noise but rather a reproducible feature of these measurements. Lateral spacing of measurements is 10 microns.

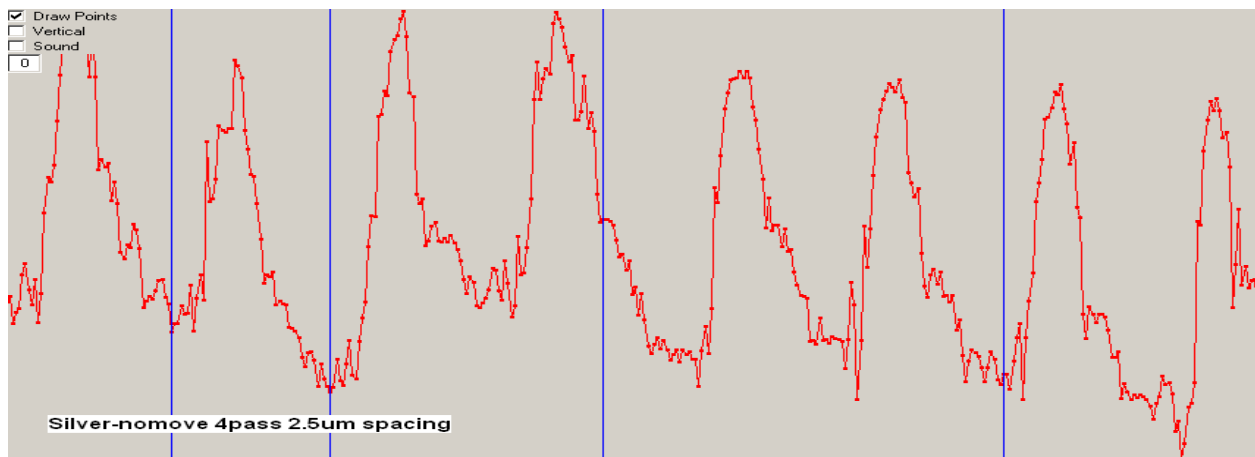


Figure 25: Confocal scan using the new MPLS180 multipoint probe. In this measurement the lateral spacing of measurements is 2.5 microns. The systematic variation of depth on the scale of a few points indicates the presence of small surface features.



Figure 26: First generation confocal probe deployed in a disc scanning configuration. Probe is tilted in order to optimize probe measurement rate for a steep groove wall.

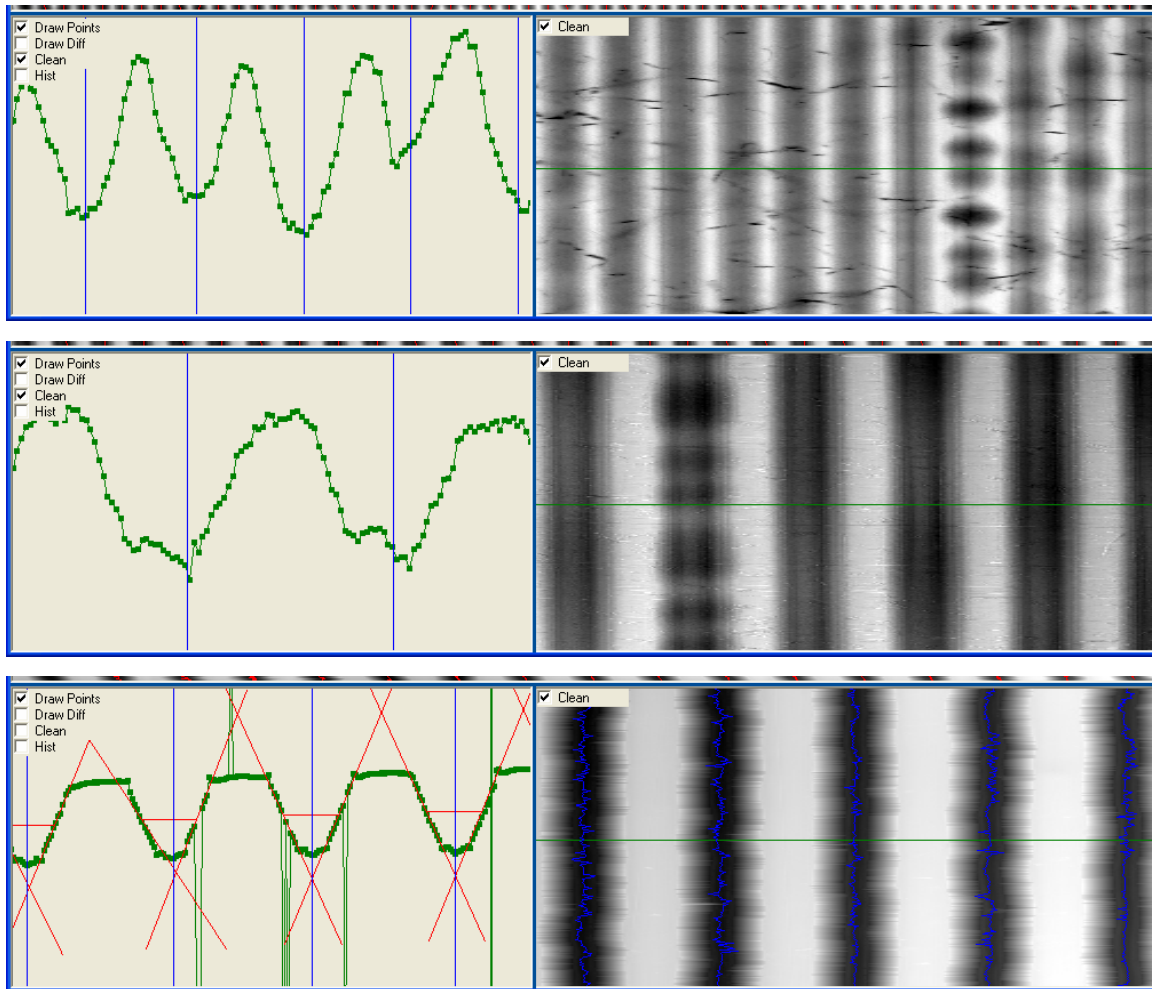


Figure 27: Examples of condition assessment. Top left shows a small region of the groove profile of a wax fieldwork cylinder. In this case the groove profile is rather typical. Top right show a grayscale image which maps intensity to surface depth measured by the confocal scanner. The vertical tracks are segments of the groove. This sample contains a large number of impressions due to fibers which may have been in contact with the cylinder in storage. These impressions could degrade the audio information stored in the surface. Middle images are another cylinder of the same vintage and type which differs considerably in condition. In this case the groove profile is irregular compared to a typical cylinder. The sharp features may be due to the particular shape of the cutting tool. This cylinder appears to be rather clean as judged by the image at middle right. Lower image is based upon a scan of a shellac disc. The groove profile is measured at lower left and surface condition is documented at lower right.